



Research article

Establishment and comparison of different procedures for modeling intrauterine adhesion in rats: A preliminary study

Peng-Cheng Liu^{a,b,1}, Yu-Ting Song^{a,b,1}, Long-Mei Zhao^{a,b}, Yan-Ling Jiang^{a,b}, Jun-Gen Hu^a, Li Dong^c, Xing-li Zhou^{a,b}, Li Zhou^d, Yaxing Li^{a,b}, Jesse Li-Ling^e, Hui-Qi Xie^{a,b,*}

^a Department of Orthopedic Surgery and Orthopedic Research Institute, Laboratory of Stem Cell and Tissue Engineering, State Key Laboratory of Biotherapy, West China Hospital, Sichuan University, Chengdu, Sichuan, China

^b Frontier Medical Center, Tianfu Jincheng Laboratory, Chengdu, Sichuan, China

^c Regenerative Medicine Research Center of Topregmed, Chengdu, Sichuan, China

^d Research Core Facility of West China Hospital, Sichuan University, Chengdu, Sichuan, China

^e Department of Medical Genetics, West China Second University Hospital, Sichuan University, Chengdu, Sichuan, China

ARTICLE INFO

Keywords:

Intrauterine adhesion
Animal model
Ethanol perfusion
Chemical injury

ABSTRACT

The establishment of a stable animal model for intrauterine adhesion (IUA) can significantly enhance research on the pathogenesis and pathological changes of this disease, as well as on the development of innovative therapeutic approaches. In this study, three different modeling methods, including phenol mucilage combined mechanical scraping, ethanol combined mechanical scraping and ethanol modeling alone were designed. The morphological characteristics of the models were evaluated. The underlying mechanisms and fertility capacity of the ethanol modeling group were analyzed and compared to those of the sham surgery group. All three methods resulted in severe intrauterine adhesions, with ethanol being identified as a reliable modeling agent and was subsequently subjected to further evaluation. Immunohistochemistry and RT-PCR results indicated that the ethanol modeling group exhibited an increase in the degree of fibrosis and inflammation, as well as a significant reduction in endometrial thickness, gland number, vascularization, and endometrial receptivity, ultimately resulting in the loss of fertility capacity. The aforementioned findings indicate that the intrauterine perfusion of 95 % ethanol is efficacious in inducing the development of intrauterine adhesions in rats. Given its cost-effectiveness, efficacy, and stability in IUA formation, the use of 95 % ethanol intrauterine perfusion may serve as a novel platform for evaluating innovative anti-adhesion materials and bioengineered therapies.

1. Introduction

As an important part of the uterus, the endometrium may be divided into functional layer and basal layer, which plays a pivotal role

* Corresponding author. Department of Orthopedic Surgery and Orthopedic Research Institute, Laboratory of Stem Cell and Tissue Engineering, State Key Laboratory of Biotherapy, West China Hospital, Sichuan University, Chengdu, Sichuan, China.

E-mail address: xiehuiqi@scu.edu.cn (H.-Q. Xie).

¹ These authors have contributed equally to this work.

<https://doi.org/10.1016/j.heliyon.2024.e25365>

Received 3 August 2023; Received in revised form 4 January 2024; Accepted 25 January 2024

Available online 29 January 2024

2405-8440/© 2024 Published by Elsevier Ltd.

This is an open access article under the CC BY-NC-ND license

(<http://creativecommons.org/licenses/by-nc-nd/4.0/>).

in female reproduction. The latter is a fundamental element in female reproduction and remains intact beneath the stratum functionalis, thereby remaining unaffected by menstruation [1]. After the menstruation, the outer endometrial functional layer will regenerate from the inner basal layer [2]. However, the self-repair and renewal ability of the endometrial basal layer may be impeded by mechanical injury, infection, and other factors, ultimately leading to the development of intrauterine adhesion (IUA) [3–6]. Severe endometrial dysfunctions can be caused by IUA, including cyclic low abdominal pain, a/hypomenorrhea, abnormal placental implant, repeated abortions and secondary infertility, which negatively impacts the reproductive health and psychological well-being of women [4]. To prevent the IUA, a variety of ancillary treatment regimens have been initiated, which included placement of physical barriers, biological barriers, and estrogen/progesterone hormone therapy [5,7,8]. Despite their therapeutic benefits, these strategies are not without limitations, including uterine inflammation, infections, bleeding, perforation, and impaired endometrial receptivity. Consequently, the management and treatment of intrauterine adhesions (IUA) remains a challenging task for gynecologists [9–13]. Therefore, there is a pressing need for the development of advanced strategies to address this dilemma.

To comprehensively evaluate the effectiveness of various treatments for IUA, it is imperative to conduct animal model investigation prior to commencing clinical trials. Consequently, it is essential to establish an animal model that can accurately mirror clinical features, including tissue response, reparative effects, and mechanisms, while also being easily accessible for subsequent experimentation on endometrial restoration and anti-adhesion materials [14], to ensure high-quality outcomes and avoid unnecessary waste of research resources.

Based on these, a variety of injury methods for establishing the IUA models have been proposed, which included mechanical damage by curets or scalpels, electrical burns, chemical damages, lipopolysaccharides-induced and various combination methods [15–18]. However, the majority of these methods are intricate and unstable. Furthermore, there is a dearth of studies that have compared these models and their respective advantages and disadvantages as a platform for testing novel tissue engineering materials.

In this study, three distinct methodologies were devised to construct an animal model of intrauterine adhesions (IUA) in Sprague-Dawley (SD) rats. To construct a stable and effective IUA model, this study comprised three parts. Firstly, the efficacy of various modeling methods was evaluated by the formation of IUA. Secondly, a model which is most suitable for *in vivo* evaluation of anti-adhesion materials has been identified, and histological evaluation was carried out at various time points. Finally, the gene expression level and reproductive outcomes of the model were furtherly evaluated.

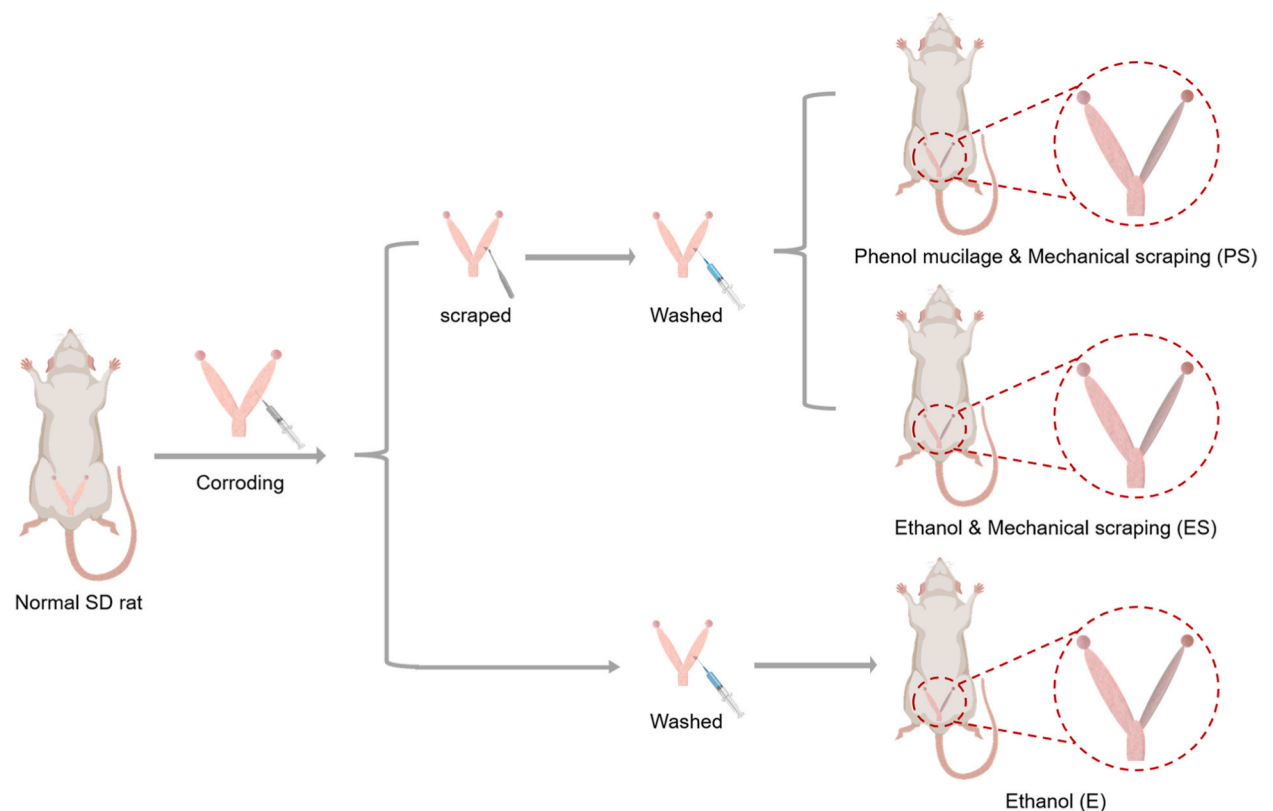


Fig. 1. Schematic diagram for the grouping of animal surgery. 1) Phenol mucilage combined with mechanical scraping (PS group), 2) ethanol combined with mechanical scraping (ES group) and 3) ethanol modeling (E group) with the endometrial damage.

2. Materials and methods

2.1. Animals

The Sichuan University Animal Care and Use Committee (20211142 A) approved all animal experiments in compliance with the National Society for Medical Research's Principles of Laboratory Animal Care. Eight-week-old mature female SD rats weighing 250 and 20 g were used in all surgical procedures (HuaFukang Biological Technologies, China). The animals were housed in groups (3–4 per cage) with free access to food (Standard feed, Huafukang Biotechnology Co., Ltd, China) and water at a temperature of $23 \pm 2^\circ\text{C}$ and light (12 h light and 12 h darkness cycle) controlled environment from one week before the surgery.

2.2. Establishment of the animal models

SD rats within dioestrus were selected for our study. As two completely separated uterine horns are present in the rats, the uterine horns were randomly modeled by 4 different methods (10 rats with 20 uterine and 5 uterine each group (Fig. 2b). Female rats with normal oestrus cycles were chosen and divided into 4 groups: 1) sham surgery (Sham group); 2) phenol mucilage combined mechanical scraping (PS group); 3) ethanol combined with mechanical scraping (ES group) and 4) ethanol modeling (E group) (Fig. 1). Ten rats were sacrificed at each time point (weeks 0, 2, 4, 8) after surgery to analyze the difference among the groups in terms of gross and endometrial morphology.

After confirmed the efficacy, stability, and long-lasting effect of 95 % ethanol as the modeling agent. Six rats from ethanol modeling (E group) and control group were subjected for more detailed histological evaluation, such as the number of endometrial glands, and area of endometrial fibrosis. To quantify the number of implanted fetuses, the modeled female animals were allowed to mate 4 and 6 weeks after surgery.

All rats were anesthetized with 1 % intraperitoneal injection of pentobarbital sodium (2 mL/kg) and supplemented when necessary. The surgeries were conducted using aseptic technique by one person to avoid the operation differences. The uterine horns were randomly assigned and operated on to minimize bias. A 2-cm vertical midline lower abdominal incision was made after disinfection with povidone iodine.

The middle segment of the uterus was clamped by two arterial clamps to create a 1.5 cm closed cavity. The intrauterine fluid was extracted by a fine needle to avoid dilution of the modeling reagent, and the modeling reagent (phenol mucilage or 95 % ethanol) was then injected into the cavity and maintained for 2 min (phenol mucilage) or 5 min (95 % ethanol), and quickly aspirated. A half-circumferential incision was made on the proximal part of the uterine, and the uterine cavity was rinsed with normal saline to avoid further erosion, additional mechanical modeling was achieved by using a scraping spoon, which was inserted and rotated inside the lumen several times until the uterine wall has become rough. The uterine horns were then placed back into the abdominal cavity after the incision was sutured. After the peritoneal cavities were flushed, the abdominal incision was closed (Fig. S1). For post-operation analgesia, ketoprofen (5 mg/kg) was administered subcutaneously.

2.3. Histological examination

After the surgery, tissue samples were collected for gross observation, histological and immunobiological evaluation, and

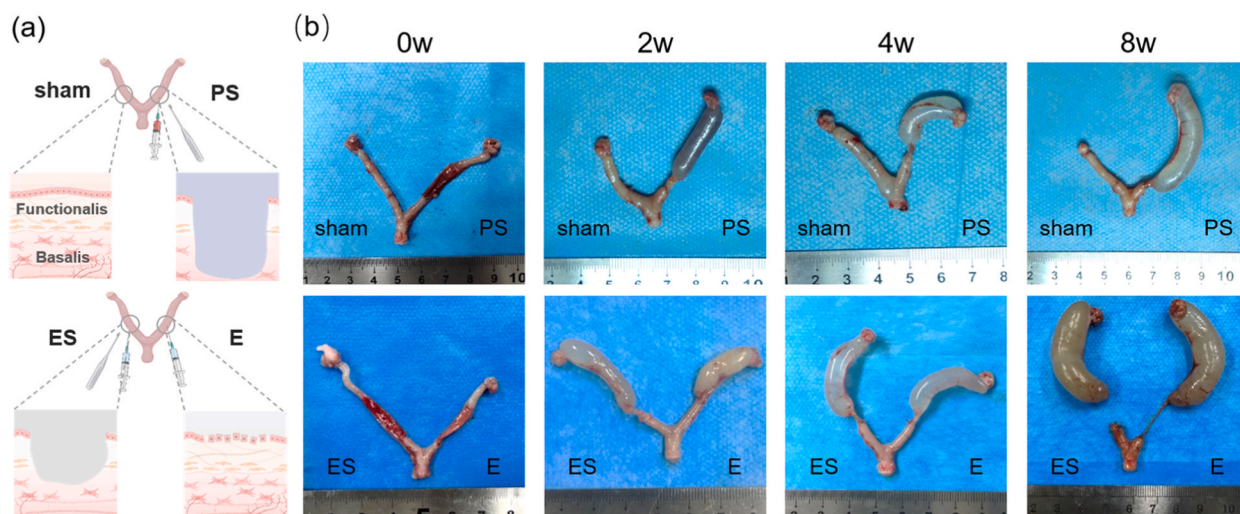


Fig. 2. Gross observation of the uterine horns after the injury at 0, 2, 4, and 8 weeks. (a) Schematic diagram of damaged uteri in different groups; (b) Representative images of the uterine horns.

immunofluorescence staining. Segments of uterus were fixed in 10 % neutral formaldehyde for 24 h, embedded in paraffin. Hematoxylin/eosin and Masson's trichrome stains were performed according to standard protocols for the observation of morphological and histological changes. The expression of α -SMA (Abcam, Cambridge, UK, 1: 1000), EpCAM (Abcam, Cambridge, UK, 1: 200), FoxA2 (Abcam, Cambridge, UK, 1: 200), and CD31 (Abcam, Cambridge, UK, 1: 1000) proteins was detected by immunohistochemistry. Images of four randomly selected fields on each slide were analyzed using Image J software 1.8.0. Histological evaluation was performed by an experienced pathologist blinded to the grouping.

2.4. Quantitative real-time PCR

4 and 6 weeks after the surgery, the uteri of all groups were removed and washed with sterile PBS. The modeling segment was collected, and total RNA was extracted by following the manufacturer's instructions. The sequences of the primers were listed in Table S1. Following the manufacturer's instructions, total RNA was extracted using the RNA Extraction Kit (Promega, USA). Quantitative QRT-PCR was performed in triplicate using TB Green® Premix Ex Taq™ II mix (Takara, Japan) on a real-time thermocycler (LC 96). Reverse transcription-PCR (RT-PCR) was performed as follows: 95 °C for 30 s, 40 cycles of 95 °C for 10 s and 60 °C for 30 s. Relative expression of the relevant genes was calculated with a $2^{-\Delta\Delta Ct}$ method as compared with that of an endogenous housekeeping gene β -actin. A 2-Ct method was used to calculate relative gene (*TGF- β 1*, *PDGF-BB*, *TIMP*, *COL1*, *MMP9*, *IL-1 β* , *IL-6*, *CD31*, *VEGF*, *Ki67*, *CK-8*, *HoxA10* and *LIF*) expression compared to an endogenous housekeeping gene β -actin.

2.5. Fertility test

To determine whether the modeled uterus may affect embryonic implantation and post-implantation development, 12 female SD rats (with 24 uterine horns) were used for the fertility test. The right uterine horn of each rat was treated as described above and assigned randomly to the sham group, 4-week group and 6-week group (6 each), while the left horn of each rat was left intact as the sham group. 4 and 6 weeks after the surgery, the female rats were mated at 1: 1 ratio with male SD rats, and were euthanized 18 days

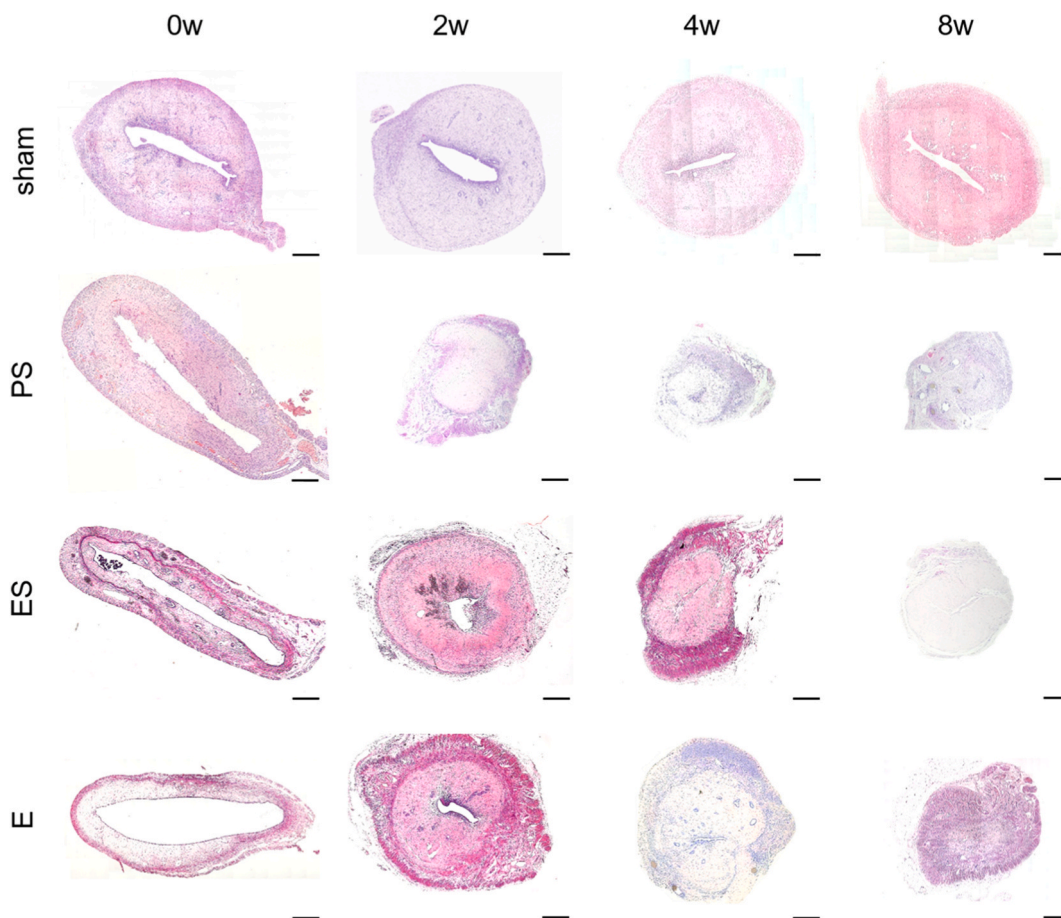


Fig. 3. Representative images of H&E-stained histological sections of the different IUA model. PS, Phenol mucilage combined with mechanical scraping; ES, ethanol combined with mechanical scraping; E, ethanol modeling group; W, weeks (Scale bar = 500 μ m).

after the appearance of vaginal plugs. The number of fetuses within each uterine horn was counted.

2.6. Statistical analysis

All values are presented as means \pm SD. SPSS 24.0 was used to perform the statistical analysis. The student's t-test or one-way ANOVA with Tukey's *post hoc* test were used to determine significance. Significant values were designated as * $P < 0.05$ or ** $P < 0.01$. All statistical images were made using the GraphPad Prism 9.0.

3. Results

3.1. Gross observation of the modeling uteri

After 8 weeks following the surgical procedure, it was observed that all rats had survived and exhibited satisfactory healing of their abdominal wounds, without any signs of infection. The sham group rats exhibited preserved uterine morphology, whereas the modeling group rats displayed elongated uteri with completely occluded and atrophic modeled segments due to adhesion. Additionally, the distal uterine horn in the modeling group exhibited enlargement due to accumulated effusion, which became increasingly evident over time. Furthermore, the uterine wall in the modeling group exhibited thinning and decreased elasticity (Fig. 2b).

3.2. Histological morphology of the modeling uteri

HE staining revealed morphological alterations in the endometrium. Following modeling, the sham group's undamaged endometrium exhibited polyloid protrusions covered by columnar epithelial cells, with enriched endometrial glands uniformly distributed throughout the basal and submucosal layers. Conversely, the endometrial epithelium was entirely compromised and shed in the PS, ES, and E groups, with some instances of deep burial within the myometrium in the PS and ES groups (Fig. 3).

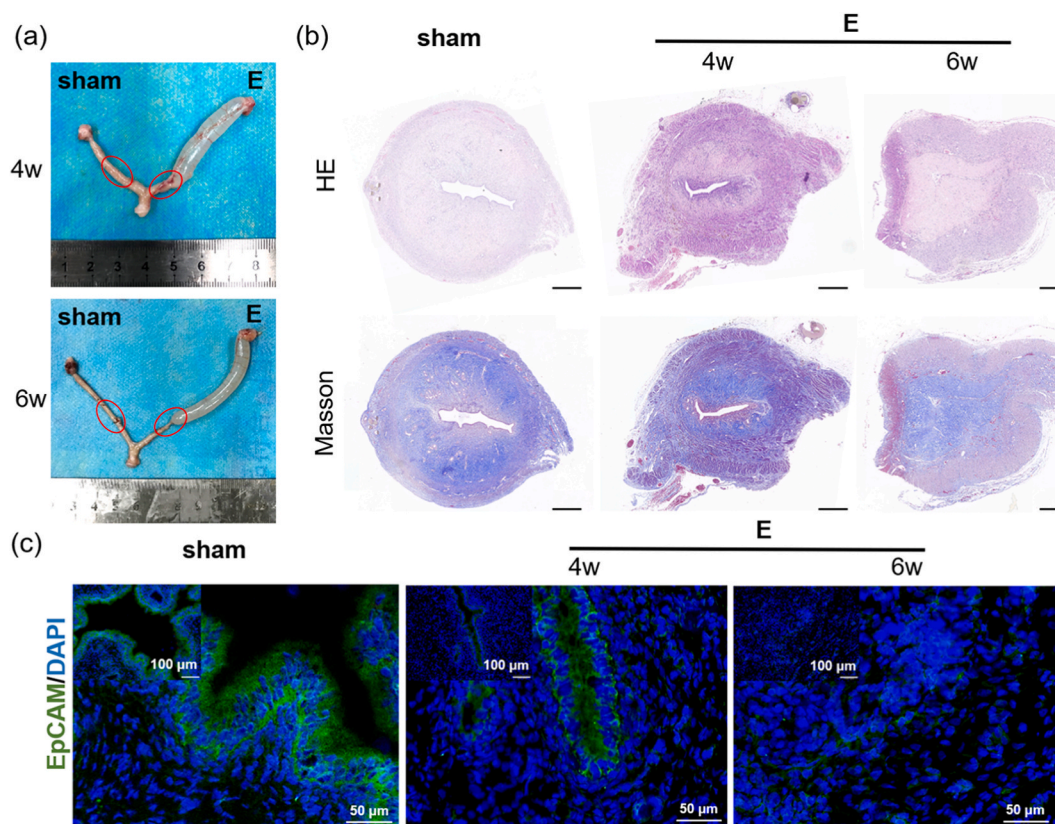


Fig. 4. Morphological, histological and immunofluorescence staining of the injured uteri damaged by 95 % ethanol corrosion method. Representative images of the uterine horns (a), HE and Masson staining (Scale bar = 500 μm) (b) and immunofluorescence staining (c) 4 and 6 weeks after the surgery. DAPI staining has 10 aggregated at the nuclei (blue), whilst EpCAM staining has aggregated at the endometrial epithelium (green). E, ethanol modeling with the endometrial damage; W, weeks. Scale bar = 100 μm (upper panel), 50 μm (bottom panel). (For interpretation of the references to colour in this figure legend, the reader is referred to the Web version of this article.)

Two weeks after the surgery, the model groups exhibited marginal or total adhesion, significant stenosis of the uterine cavity, and focal endometrial repair. The thickened uterine wall indicated extensive hyperplastic changes. Four weeks post-surgery, complete intrauterine adhesions had formed, leading to near-complete occlusion of the uterine cavity. The endometrial epithelium had almost entirely disappeared, with a significant decrease in gland number and blood vessel density. The surrounding tissue exhibited more apparent hyperplastic changes. After a period of 8 weeks post-operation, the uterine cavity was observed to have undergone complete obliteration. The modeled uterine tissue was characterized by advanced fibrosis with minimal cellular infiltration, and no discernible

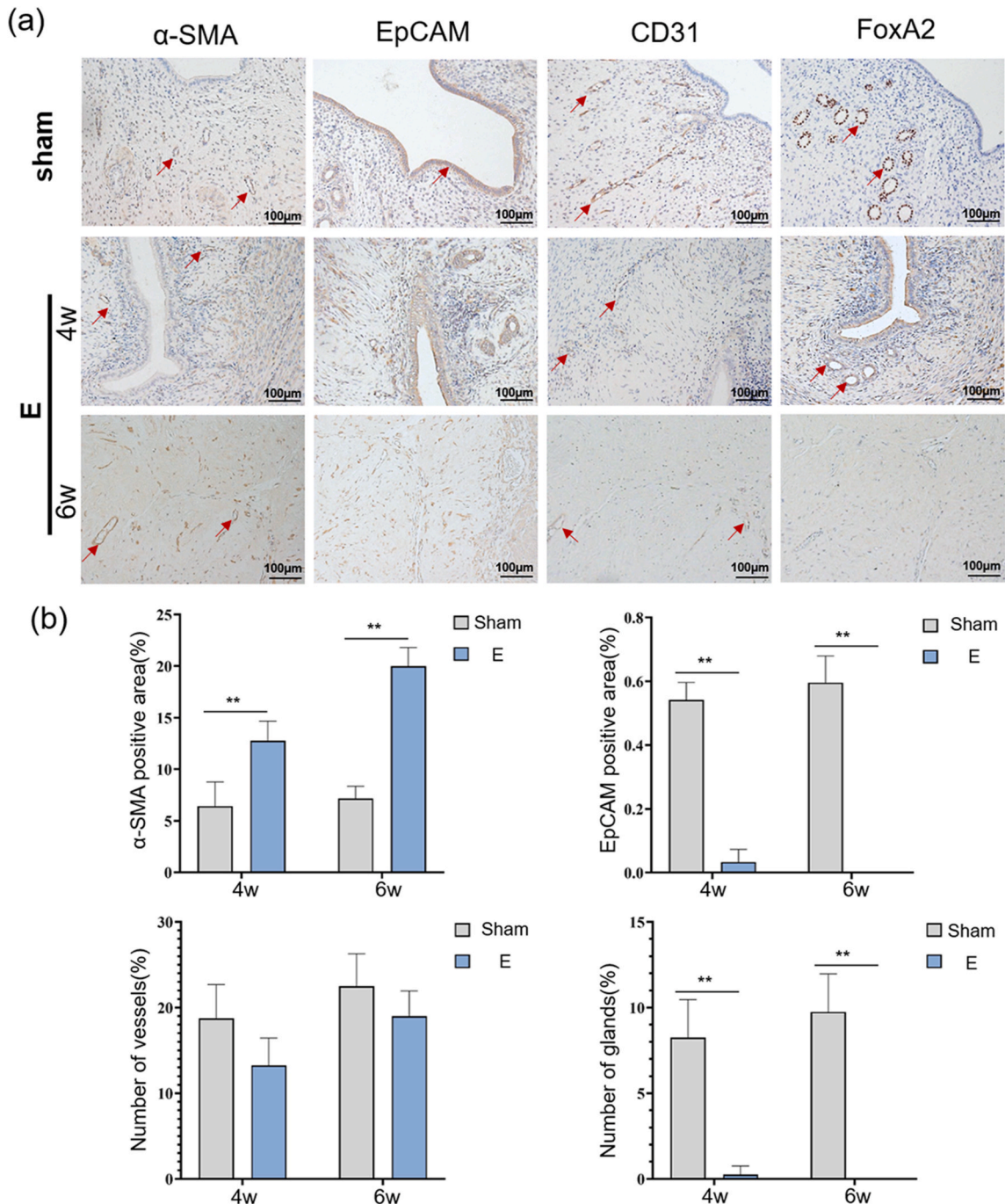


Fig. 5. Immunofluorescence staining of the injured uteri damaged by 95 % ethanol corrosion method. (a) Representative immunohistochemical images; (b) statistical histogram of α-SMA, EpCAM and CD31 expression, and number of glands at 4 and 6 weeks. Arrows have indicated the blood vessels, epithelium and glands, respectively. E, ethanol modeling with the endometrial damage; W, weeks. Scale bar = 100 μm *P < 0.05 and **P < 0.01.

blood vessels or glands were detected. These findings suggest that the rats had lost their capacity for endometrial epithelial regeneration and were unable to autonomously restoration.

3.3. 95 % ethanol corrosion model

Although the three aforementioned methods could all cause severe IUA, the mechanical method is typically constrained by factors such as personnel expertise, surgical equipment, and experimental variables. Therefore, the outcomes of these methods are characterized by poor consistency and repeatability. Consequently, we have opted to employ the 95 % ethanol corrosion method in our subsequent investigations.

Four weeks after the operation, the sham group's uterine horn exhibited a restoration of normal morphology and histology characteristics. Conversely, the injured area displayed stenosis, leading to an accumulation of effusion and elongation of the distal uterine (Fig. 4a). The endometrial epithelium was remarkably reduced and obvious fibrosis was observed (Fig. 4b). At six weeks post-surgery, the uterine in the E group was entirely occluded, with a significant increase in effusion accumulation and a remarkable enlargement of the distal uterus. The uterine wall exhibited a decrease in thickness and elasticity (Fig. 4a and b). Additionally, the endometrial epithelium was barely visible and advanced fibrosis presented, suggesting that the rats had lost their ability for endometrial epithelial regeneration and could not repair the uterine cavity damage by themselves (Fig. 4c).

Considering its cost-effectiveness, efficacy, and stability in IUA formation, ethanol was regarded as a more appropriate modeling agent and subsequently subjected to further evaluation. Immunohistochemical staining was carried out on the tissues harvested from

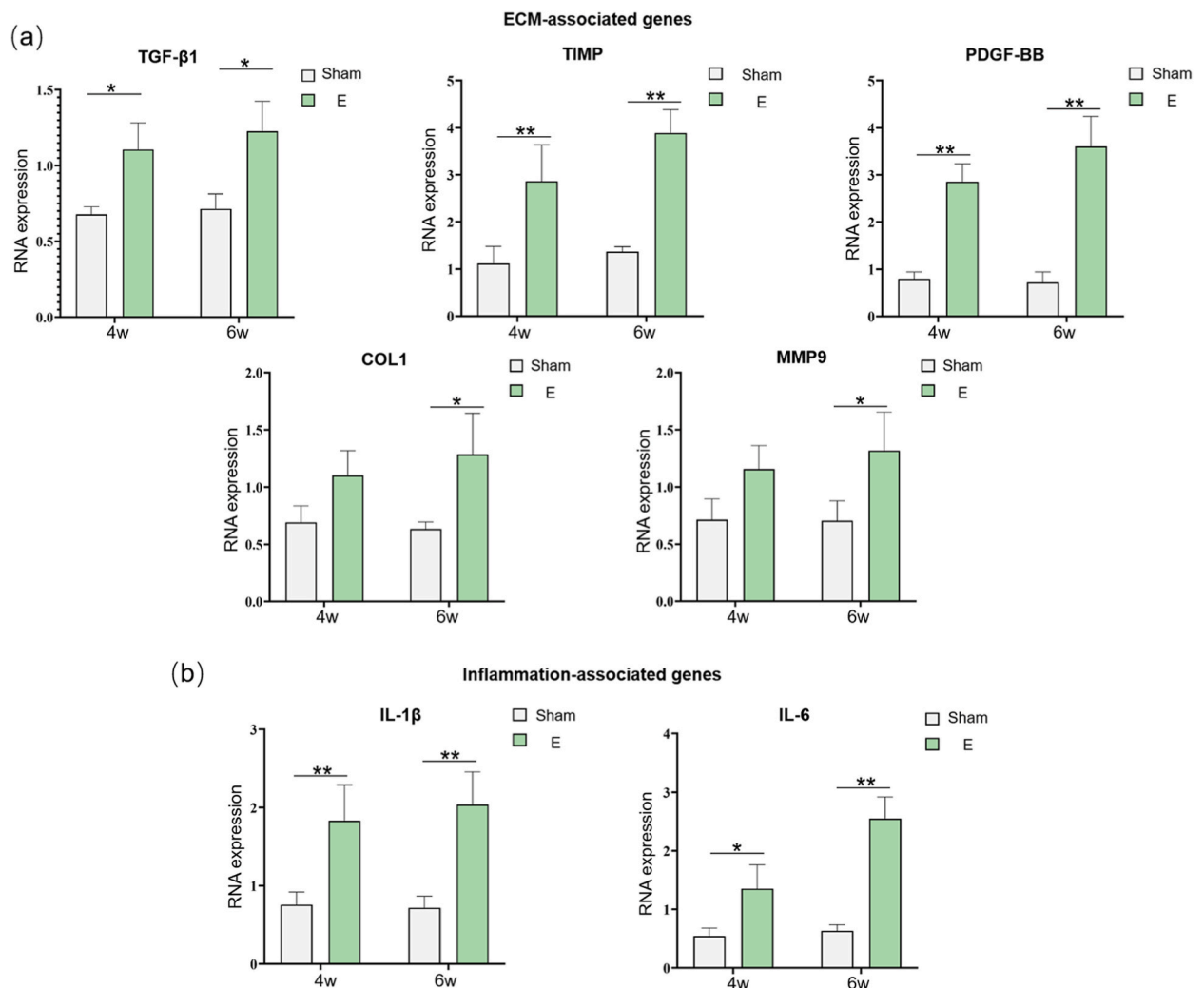


Fig. 6. Analysis of the fibrosis and inflammatory of the injured uteri damaged by 95 % ethanol corrosion method. (a) The mRNA level of the ECM deposition-related genes (TGF-β1, PDGF-BB, TIMP, COL1 and MMP9), and (b) inflammatory-related genes (IL-1β and IL-6) in the tissue from the repair area at 4 and 6 weeks postoperatively were detected by qRT-PCR. E, ethanol modeling with the endometrial damage; W, weeks. *P < 0.05 and **P < 0.01.

the sham and the E group at 4 and 6 weeks after the surgery (Fig. 5a). The α -SMA was used to evaluate the extent of tissue fibrosis. EpCAM was used to label the endometrial epithelium, and CD31 and FoxA2 were used to detect the blood vessels and glands, respectively. As shown, the E group expressed significantly more α -SMA and less EpCAM and FoxA2 at both 4 and 6 weeks, while there was no significant difference in the number of blood vessels between the two groups (Fig. 5b).

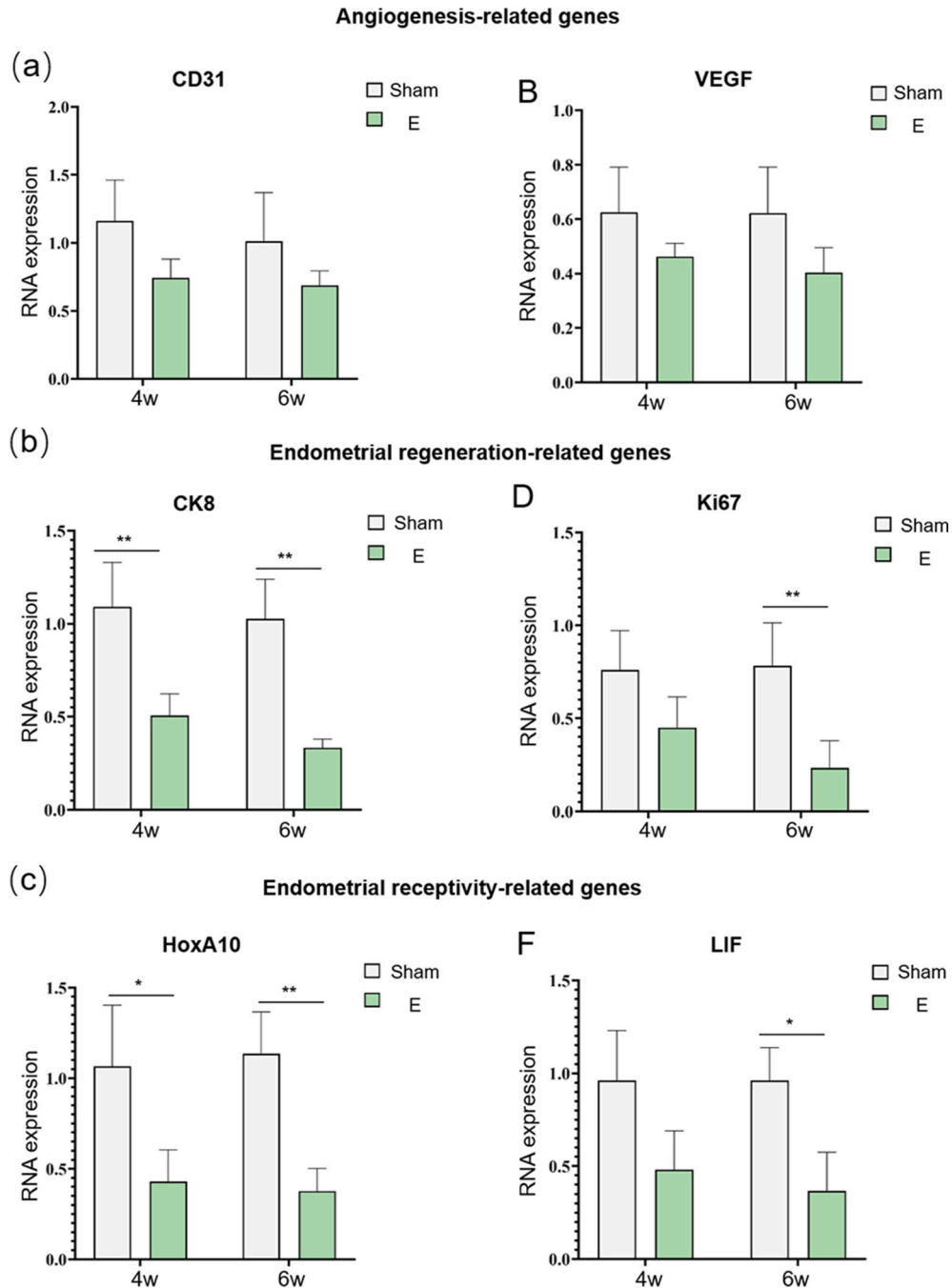


Fig. 7. Analysis of the vascular, epithelial, and endometrial receptivity of the injured uteri damaged by 95 % ethanol corrosion method. (a) The mRNA expression of angiogenesis-related genes (CD31 and VEGF), (b) endometrial regeneration-related genes (Ki67 and CK8), and (c) endometrial receptivity-related genes (HoxA10 and LIF) in tissues from the repair area at 4 and 6 weeks postoperatively were detected by qRT-PCR. * $P < 0.05$ and ** $P < 0.01$.

3.4. Molecular mechanisms of ethanol modeling

To clarify the underlying mechanism of ethanol modeling, changes in the expression of certain genes associated with ECM deposition, inflammation, angiogenesis, endometrial regeneration and endometrium receptivity were determined, receptivity. As shown in Fig. 6, compared with the sham group, genes (*TGF- β 1*, *COL1*, *TIMP*, *MMP9*, *PDGF-BB*) related to ECM deposition were significantly upregulated at 4 and 6 weeks in the E group (Fig. 6a). Inflammatory reactions were confirmed by the QRT-PCR results. The mRNA level of both *IL-1 β* and *IL-6* have become significantly different from that of the sham group and E group ($P < 0.01$) (Fig. 6b).

The vascular endothelial cells regeneration was confirmed by analyzing angiogenesis-related genes. No significant difference was found in the mRNA levels of the CD31 and VEGF genes between the two groups (Fig. 7a). Genes involved in endometrial and gland proliferation were monitored to evaluate endometrial regeneration. Compared to the sham group, Ki67 and CK-8 mRNA levels were significantly reduced in the E group after 4 weeks ($P < 0.01$) and 6 weeks ($P < 0.01$, $P < 0.05$, respectively), respectively (Fig. 7b). The expression of endometrial receptivity-related genes was also altered. HoxA10 and LIF are crucial determinants of uterine receptivity. At 4 and 6 weeks after surgery, the expression level of HoxA10 mRNA was significantly downregulated in the E group, while LIF mRNA only showed a significant difference 6 weeks after surgery ($P < 0.05$) (Fig. 7c).

3.5. Pregnancy outcome

To assess the effect of IUA on the fertility of female rats, pregnancy outcomes were evaluated after modeling. As shown, the E group failed to conceive due to severe IUA, and the fetal rates in the E group (0 %) were lower than those in the sham group (83 %) (Fig. 8a and b).

4. Discussion

The selection of appropriate animal models and identification of effective methodologies for establishment are important in the investigation of human diseases [19]. The utilization of

uncomplicated, consistent, and efficient animal models can be beneficial for the development of novel materials for endometrial restoration and anti-adhesion. In this study, three distinct

approaches to establish a rat model of IUA, and the feasibility of each method was assessed at

multiple time points. A reproducible and viable method for modeling IUA using 95 % ethanol was established through comparative analysis.

Animal models of intrauterine adhesions (IUA) have been established using various species, such as mice, rats, New Zealand white rabbits, beagles, and rhesus monkeys, with different modeling approaches [18,20–24]. Among these options, the rat has emerged as the most commonly used model due to its distinct genetic background, robust reproductive capabilities, uncomplicated dietary needs, cost-effectiveness, spontaneous ovulation, and regular estrous cycle. Moreover, the rat's double uterus and non-interfering uterine horns make it an ideal animal model for reducing experimental bias [25].

Various modeling methods for IUA have been reported, including mechanical injury, infection, electrothermal injury, and chemical injury. In recent years, researchers have developed animal models of IUA by infecting them with copper wire or lipopolysaccharide

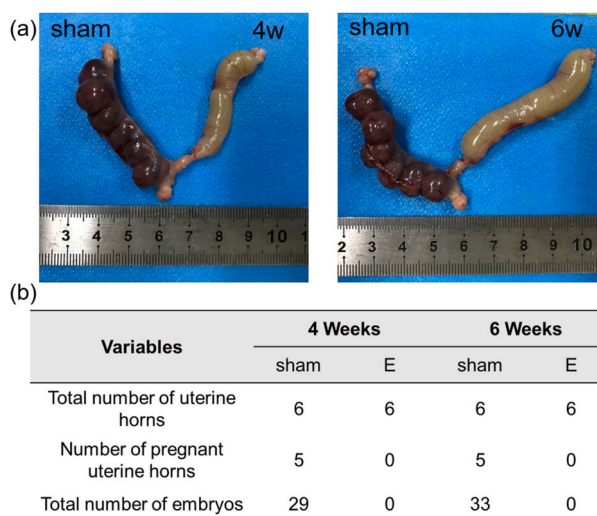


Fig. 8. The fertility outcomes. (a). The gross observation of fertility results between control and E group at 4 and 6 weeks, (b). Quantitative results of fertility experiment.

cotton thread [17,26,27]. However, such foreign bodies need to be removed from the uterine cavity, and the procedure is complex. Furthermore, this method has aimed to simulate the IUA caused by IUD infection, which may not be applicable to all studies. Consequently, our study primarily focuses on assessing the effectiveness of mechanical injury and chemical etching techniques.

Mechanical injury is caused by scratching the endometrium with surgical instruments [28,29], which aligns more closely with the clinical etiology of IUA. However, the establishment of models through this method is limited by personal expertise, surgical instrumentation, and experimental conditions. These constraints have historically led to inconsistent and non-reproducible results [16]. As previously explained, dual-injury methods have not shown significant advancements compared to other methods in successful modeling. Furthermore, their execution is complex, making them less suitable for recommendation. On the other hand, chemical injury can erode the uterine wall using chemical reagents, and the degree of severity can be easily controlled. This method offers advantages in terms of consistency and repeatability [16]. Thus, an increasing number of studies have begun to choose chemical methods.

Among the chemical reagents commonly used, phenol mucilage and ethanol are frequently employed either separately or in combination with mechanical methods [30]. Previous research has compared various techniques, including ethanol perfusion, thermal stripping, mechanical injury, and mechanical co-infection, and has found that ethanol perfusion exhibits the highest stability [31]. This study also compared the modeling effect of these reagents alone or in combination. Based on gross observation and HE staining, all three methods resulted in severe intrauterine adhesions (Fig. 3), confirming the reliability of ethanol as a modeling agent. In contrast, the accessibility and cost-effectiveness of ethanol are superior to those of phenol mucilage. Therefore, ethanol appeared to be a more suitable modeling agent and was selected for further evaluation.

Ethanol perfusion could cause damage to the endometrium, and ultimately contribute to the formation of stable adhesion. Previous studies have identified endometrial thickness, the number of endometrial glands, fibrosis area, and the presence of adhesions as important indicators for evaluating the formation of the IUA animal model [4,32–35]. When the damaged endometrium cannot be effectively repaired, it results in the replacement of the endometrial stroma with a significant amount of fibrous tissue. Our findings showed a significantly higher degree of fibrosis, near absence of endometrium, and more evident reduction in gland count in our IUA model compared to the sham group at both 4- and 6-weeks post-surgery. Based on our observations, intrauterine adhesions caused by ethanol are irreparable on their own, but can be reversed using biomaterial scaffolds, as demonstrated in our previous study [20]. This finding could serve as an important reference point for utilizing biomaterials in the treatment and prevention of intrauterine adhesion within animal models.

The excessive deposition of extracellular matrix (ECM) collagen represents a significant alteration in the fibrous uterine, as previously reported [36–38]. It has been reported that *TGF-β1* and *PDGF-BB* can significantly promote the expression of COL1 and α -SMA, which play an important role in the process of fibrosis [30,39–42]. *TIMP* plays a key role in the formation and dissolution of fibrosis [38,43,44]. In addition, it has been reported that MMP-9, the downstream target gene of TGF- β 1, plays an important role in endometrial remodeling important role in endometrial remodeling, and is involved in the fibrosis process through degrading and reorganizing ECM [45–48]. MMP-9 can participate in the occurrence of IUA through Mesenchymal transition (EMT) and promote endometrial fibrosis [49,50]. Thus, we conducted QRT-PCR analysis to assess the expression levels of TGF- β 1, PDGF-BB, TIMP, MMP-9, and COL1 in the modeled segments. Our findings indicate that the extent of uterine fibrosis following alcohol corrosion increased over time post-surgery, which is in line with the clinicopathological alterations observed in IUA [51,52].

Inflammation and vascular damage are also important causes for endometrial fibrosis [7,53,54]. Previous studies have shown that inflammation may hinder the regeneration of injured endometrium and activate a number of downstream pathways to further aggravate the fibrosis [55]. Therefore, we employed immunohistochemistry and QRT-PCR to assess genes and proteins linked to inflammation (IL1 β and IL6) and vascularization (CD31 and VEGF). The findings indicated that the implementation of the IUA model led to heightened inflammation, aligning with the observed pathological alterations in human IUA. For Ki67 is a nuclear antigen closely associated with cell proliferation [56], and CK8 is an indicator that can indirectly reflect changes in the endometrial epithelium [57], we have further detected the expression levels and verified the impaired capacity of endometrial epithelium regeneration.

In addition, unlike prior research, our study incorporates an appraisal of uterine function as a metric for assessing the animal model. The assessment of uterine function loss encompasses two facets, namely endometrial receptivity and fertility evaluation. Endometrial receptivity pertains to the capacity of the endometrium to permit and facilitate embryo implantation [58]. HoxA10 and LIF are widely used as the indicators of endometrial receptivity [59]. HoxA10 is a critical regulatory factor in embryo implantation, which involved in the embryogenesis of the uterus and embryo implantation via regulation of downstream genes [60]. LIF is a pleiotropic cytokine with a critical dual function in initiates endometrial decidualization and embryonic development [61–63]. The QRT-PCR results indicate that our methods have the potential to decrease the endometrial receptivity of rats. Subsequently, we assessed the pregnancy outcomes following modeling. Our findings demonstrate that the ethanol modeling rats were unable to conceive at any point due to the presence of severe intrauterine adhesions. The aforementioned evidence suggests that our model successfully induced stable uterine adhesions that were not self-restorable in rats. In summary, the procedure of ethanol corrosion method has a noteworthy impact on various endometrial parameters such as thickness, gland count, degree of fibrosis, and pregnancy outcomes. Taken together, ethanol corrosion has a significant effect on the endometrial thickness, number of glands, degree of fibrosis and pregnancy outcome, which has confirmed the desirability of ethanol instillation as an IUA modelling procedure.

This study has certain limitations. Firstly, this approach is readily applicable to small animal models, as thin endometrium guarantees efficacy and stability in a short time. Secondly, the rare occurrence of chemically induced uterine injury may not fully replicate the pathogenesis of clinical IUA. Therefore, this model is more suitable for in vivo assessment of antiadhesion biomaterials or stem cell-based therapies, rather than for investigating the pathogenesis of IUA. Our subsequent studies will focus on investigate its interrelated mechanism in the prevention of IUA by tissue engineering scaffolds.

5. Conclusion

Our modeling approach is capable of effectively establishing stable and long-lasting results. This method is not only cost-effective but also reliable, making it suitable for preclinical evaluations of therapeutic strategies, including anti-adhesion materials and bio-engineered therapies.

Funding

This study was supported by the Frontiers Medical Center, Tianfu Jincheng Laboratory Foundation (TFJC2023010002), Med-X Center for Materials, Sichuan University (MCM202104), and the “1.3.5” Project for Disciplines of Excellence, the West China Hospital, Sichuan University (ZYJC18002) to Xie Huiqi.

Data availability statement

All data generated or analyzed during this study are included in this article. Raw files and additional information are may be available by the corresponding author upon reasonable request.

CRedit authorship contribution statement

Peng-Cheng Liu: Writing – original draft, Methodology, Formal analysis, Data curation. **Yu-Ting Song:** Writing – original draft, Methodology, Formal analysis. **Long-Mei Zhao:** Methodology, Data curation. **Yan-Ling Jiang:** Methodology, Data curation. **Jun-Gen Hu:** Software, Methodology. **Li Dong:** Methodology. **Xing-li Zhou:** Resources, Methodology. **Li Zhou:** Supervision, Methodology. **Yaxing Li:** Methodology, Investigation. **Jesse Li-Ling:** Writing – review & editing, Supervision, Methodology. **Hui-Qi Xie:** Writing – review & editing, Validation, Supervision, Project administration, Funding acquisition, Formal analysis, Data curation, Conceptualization.

Declaration of competing interest

The authors declare that they have no known competing financial interests or personal relationships that could have appeared to influence the work reported in this paper.

Acknowledgment

None.

Appendix A. Supplementary data

Supplementary data to this article can be found online at <https://doi.org/10.1016/j.heliyon.2024.e25365>.

References

- [1] C.A. Salazar, K. Isaacson, S. Morris, A comprehensive review of Asherman's syndrome: causes, symptoms and treatment options, *Curr. Opin. Obstet. Gynecol.* 29 (4) (2017) 249–256.
- [2] J. Vallvé-Juanico, S. Houshdaran, L.C. Giudice, The endometrial immune environment of women with endometriosis, *Hum. Reprod. Update* 25 (5) (2019) 564–591.
- [3] J.G. Asherman, Amenorrhoea traumatica (atretica), *J. Obstet. Gynaecol. Br. Emp.* 55 (1) (1948).
- [4] E. Dreisler, J.J. Kjer, Asherman's syndrome: current perspectives on diagnosis and management, *Int. J. Womens. Health.* 11 (2019) 191–198.
- [5] C.M. March, Management of Asherman's syndrome, *Reprod. Biomed. Online* 23 (1) (2011) 63–76.
- [6] H. Zhu, Y. Pan, Y. Jiang, J. Li, Y. Zhang, S. Zhang, Activation of the Hippo/TAZ pathway is required for menstrual stem cells to suppress myofibroblast and inhibit transforming growth factor beta signaling in human endometrial stromal cells, *Hum. Reprod.* 34 (4) (2019) 635–645.
- [7] D. Yu, Y.M. Wong, Y. Cheong, E. Xia, T.C. Li, Asherman syndrome—one century later, *Fertil. Steril.* 89 (4) (2008) 759–779.
- [8] B. Hooker, M. Lemmers, A.L. Thurkow, M.W. Heymans, B.C. Opmeer, H.A. Brolmann, B.W. Mol, J.A. Huirne, Systematic review and meta-analysis of intrauterine adhesions after miscarriage: prevalence, risk factors and long-term reproductive outcome, *Hum. Reprod. Update* 20 (2) (2014) 262–278.
- [9] X. Zhang, W. Liu, Y. Zhou, J. Qiu, Y. Sun, M. Li, Y. Ding, Q. Xi, Comparison of therapeutic efficacy of three methods to prevent re-adhesion after hysteroscopic intrauterine adhesion separation: a parallel, randomized and single-center trial, *Ann. Palliat. Med.* 10 (6) (2021) 6804–6823.
- [10] L.Z. Pan, Y. Wang, X. Chen, A randomized controlled study on an integrated approach to prevent and treat re-adhesion after transcervical resection of moderate-to-severe intrauterine adhesions, *Clinics* 76 (2021) e1987.
- [11] B.A. Tjokroprawiro, Laparotomy for abdominal adhesion and removal of intrauterine device from anatomically distorted uterus due to adhesion in a 43-year-old woman with 3 previous cesarean sections, *Am. J. Case. Rep.* 22 (2021) e934530.
- [12] M.L. Cheung, S. Rezaei, J.M. Jackman, N.D. Patel, B.Z. Bernaba, O. Hakimian, D. Nuritdinova, C.L. Turley, R. Mercado, T. Takeshige, S.M. Reddy, P.N. Fuller, C. E. Hendersen, Retained intrauterine device (IUD): triple case report and review of the literature, *Case. Rep. Obstet. Gynecol.* (2018) 9362962, 2018.
- [13] Y. Chen, L. Liu, Y. Luo, M. Chen, Y. Huan, R. Fang, Effects of aspirin and intrauterine balloon on endometrial repair and reproductive prognosis in patients with severe intrauterine adhesion: a prospective cohort study, *BioMed Res. Int.* 2017 (2017) 8526104.

- [14] Y. Jahanbani, S. Davaran, M. Ghahremani-Nasab, L. Aghebati-Maleki, M. Yousefi, Scaffoldbased tissue engineering approaches in treating infertility, *Life Sci.* 240 (2020) 117066.
- [15] Q. Feng, B. Gao, X. Zhao, H. Huang, S. Yi, L. Zou, X. Liu, M. Xue, D. Xu, Establishment of an animal model of intrauterine adhesions after surgical abortion and curettage in pregnant rats, *Ann. Transl. Med.* 8 (4) (2020) 56.
- [16] S. Zhang, Y. Sun, D. Jiang, T. Chen, R. Liu, X. Li, Y. Lu, L. Qiao, Y. Pan, Y. Liu, J. Lin, Construction and optimization of an endometrial injury model in mice by transcervical ethanol perfusion, *Reprod. Sci.* 28 (3) (2021) 693–702.
- [17] F. Liu, Z.-J. Zhu, P. Li, Y.-L. He, Creation of a female rabbit model for intrauterine adhesions using mechanical and infectious injury, *J. Surg. Res.* 183 (1) (2013) 296–303.
- [18] X.X. Xu, L.B. Cao, Z. Wang, Z. Xu, B.Q. Zhang, S.L. Wu, S.S. Qi, L. Yan, Z.J. Chen, Creation of a rabbit model for intrauterine adhesions using electrothermal injury, *J. Zhejiang Univ. - Sci. B.* 19 (5) (2018) 383–389.
- [19] R. A'la, A.Y. Wijaya, H. Susilowati, S. Kuncorojakti, J. Diyantoro Rahmahani, F.A. Rantam, Inactivated SARS-CoV-2 vaccine candidate immunization on non-human primate animal model: B-cell and T-cell responses immune evaluation, *Heliyon* 9 (7) (2023) e18039.
- [20] Y.T. Song, L. Dong, J.G. Hu, P.C. Liu, Y.L. Jiang, L. Zhou, M. Wang, J. Tan, Y.X. Li, Q.Y. Zhang, C.Y. Zou, X.Z. Zhang, L.M. Zhao, R. Nie, Y. Zhang, J. Li-Ling, H. Q. Xie, Application of genipin-crosslinked small intestine submucosa and urine-derived stem cells for the prevention of intrauterine adhesion in a rat model, *Composites, Part B* 250 (2023) 110461.
- [21] B. Li, Q. Zhang, J. Sun, D. Lai, Human amniotic epithelial cells improve fertility in an intrauterine adhesion mouse model, *Stem Cell Res. Ther.* 10 (1) (2019) 257.
- [22] Y. Yao, R. Chen, G. Wang, Y. Zhang, F. Liu, Exosomes derived from mesenchymal stem cells reverse EMT via TGF- β 1/Smad pathway and promote repair of damaged endometrium, *Stem Cell Res. Ther.* 10 (1) (2019) 225.
- [23] X. Zhang, G. Chen, Y. Wang, L. Fan, Y. Zhao, Arrowhead composite microneedle patches with anisotropic surface adhesion for preventing intrauterine adhesions, *Adv. Sci.* 9 (12) (2022) e2104883.
- [24] B. Larsson, G. Aström, S. Einarsson, L. Rydén, I. Granberg-Ohman, B.A. Lindhe, The possible risks of a copper and an inert intrauterine device situated in the abdominal cavity: an experimental study in pigs and dogs, *Fertil. Steril.* 36 (2) (1981) 229–231.
- [25] Y.T. Song, P.C. Liu, J. Tan, C.Y. Zou, Q.J. Li, J. Li-Ling, H.Q. Xie, Stem cell-based therapy for ameliorating intrauterine adhesion and endometrium injury, *Stem Cell Res. Ther.* 12 (1) (2021) 556.
- [26] W.B. Qi, L.J. Xu, S.D. Zhao, J.H. Zheng, Y.P. Tian, X.J. Qi, X.H. Huang, J.K. Zhang, Controlled releasing of SDF-1 α in chitosan-heparin hydrogel for endometrium injury healing in rat model, *Int. J. Biol. Macromol.* 143 (2020) 163–172.
- [27] L. Li, J. Shi, Q.F. Zhang, J. Yan, L.Y. Yan, F. Shen, J. Qiao, H.L. Feng, Effect of curettage and copper wire on rabbit endometrium: a novel rabbit model of endometrial mechanical injury, *Chin. Med. J.* 124 (11) (2011) 1708–1713.
- [28] L. Xin, X. Lin, Y. Pan, X. Zheng, L. Shi, Y. Zhang, L. Ma, C. Gao, S. Zhang, A collagen scaffold loaded with human umbilical cord-derived mesenchymal stem cells facilitates endometrial regeneration and restores fertility, *Acta Biomater.* 92 (2019) 160–171.
- [29] B. Wang, C. Feng, J. Dang, Y. Zhu, X. Yang, T. Zhang, R. Zhang, J. Li, J. Tang, C. Shen, L. Shen, J. Dong, X. Zhang, Preparation of fibroblast suppressive poly(ethylene glycol)-b-poly(l-phenylalanine)/poly(ethylene glycol) hydrogel and its application in intrauterine fibrosis prevention, *ACS Biomater. Sci. Eng.* 7 (1) (2021) 311–321.
- [30] U. Salma, M. Xue, M.S. Ali Sheikh, X. Guan, B. Xu, A. Zhang, L. Huang, D. Xu, Role of transforming growth factor- β 1 and smads signaling pathway in intrauterine adhesion, *Mediat. Inflamm.* (2016) 4158287, 2016.
- [31] L. Sun, S. Zhang, Q. Chang, J. Tan, Establishment and comparison of different intrauterine adhesion modelling procedures in rats, *Reprod. Fertil. Dev.* 31 (8) (2019) 1360–1368.
- [32] E.A. Evans-Hoeker, S.L. Young, Endometrial receptivity and intrauterine adhesive disease, *Semin. Reprod. Med.* 32 (5) (2014) 392–401.
- [33] X. Santamaria, K. Isaacson, C. Simón, Asherman's Syndrome: it may not be all our fault, *Hum. Reprod.* 33 (8) (2018) 1374–1380.
- [34] A. Foix, R.O. Bruno, T. Davison, B. Lema, The pathology of postcurettage intrauterine adhesions, *Am. J. Obstet. Gynecol.* 96 (7) (1966) 1027–1033.
- [35] A. Conforti, C. Alviggi, A. Mollo, G. De Placido, A. Magos, The management of Asherman syndrome: a review of literature, *Reprod. Biol. Endocrinol.* 11 (2013) 118.
- [36] P.J. Wolters, C.J. Le Saux, K. Atabai, Age-dependent regulation of cell-mediated collagen turnover, *JCI. Insight.* 5 (10) (2020).
- [37] S. Liu, X. Huang, Y. Liu, D. Song, Y. Xiao, Functional analysis of miRNAs combined with TGF- β 1/Smad3 inhibitor in an intrauterine rat adhesion cell model, *Mol. Cell. Biochem.* 470 (1–2) (2020) 15–28.
- [38] X. Ouyang, S. You, Y. Zhang, C. Zhang, G. Zhang, X. Shao, F. He, L. Hu, Transplantation of human amnion epithelial cells improves endometrial regeneration in rat model of intrauterine adhesions, *Stem Cell. Dev.* 29 (20) (2020) 1346–1362.
- [39] G. Gabbiani, The myofibroblast in wound healing and fibrocontractive diseases, *J. Pathol.* 200 (4) (2003) 500–503.
- [40] P. Zymek, M. Bujak, K. Chatila, A. Cieslak, G. Thakker, M.L. Entman, N.G. Frangogiannis, The role of platelet-derived growth factor signaling in healing myocardial infarcts, *J. Am. Coll. Cardiol.* 48 (11) (2006) 2315–2323.
- [41] H. Matsumoto, K. Nasu, M. Nishida, H. Ito, S. Bing, I. Miyakawa, Regulation of proliferation, motility, and contractility of human endometrial stromal cells by platelet-derived growth factor, *J. Clin. Endocrinol. Metab.* 90 (6) (2005) 3560–3567.
- [42] H. Matsumoto, K. Nasu, M. Nishida, H. Ito, S. Bing, I. Miyakawa, Regulation of proliferation, motility, and contractility of human endometrial stromal cells by platelet-derived growth factor, *J. Clin. Endocrinol. Metab.* 90 (6) (2005) 3560–3567.
- [43] S.K. Das, D.M. Vasudevan, Genesis of hepatic fibrosis and its biochemical markers, *Scand. J. Clin. Lab. Invest.* 68 (4) (2008) 260–269.
- [44] J.P. Iredale, Tissue inhibitors of metalloproteinases in liver fibrosis, *Int. J. Biochem. Cell Biol.* 29 (1) (1997) 43–54.
- [45] J.L. Skinner, S.C. Riley, A.E. Gebbie, A.F. Glasier, H.O. Critchley, Regulation of matrix metalloproteinase-9 in endometrium during the menstrual cycle and following administration of intrauterine levonorgestrel, *Hum. Reprod.* 14 (3) (1999) 793–799.
- [46] S.X. Bai, Y.L. Wang, L. Qin, Z.J. Xiao, R. Herva, Y.S. Piao, Dynamic expression of matrix metalloproteinases (MMP-2, -9 and -14) and the tissue inhibitors of MMPs (TIMP-1, -2 and -3) at the implantation site during tubal pregnancy, *Reproduction* 129 (1) (2005) 103–113.
- [47] H. Zhao, Y. Dong, X. Tian, T.K. Tan, Z. Liu, Y. Zhao, Y. Zhang, D. Harris, G. Zheng, Matrix metalloproteinases contribute to kidney fibrosis in chronic kidney diseases, *World J. Nephrol.* 2 (3) (2013) 84–89.
- [48] M. Zeisberg, M. Khurana, V.H. Rao, D. Cosgrove, J.P. Rougier, M.C. Werner, C.F. Shield 3rd, Z. Werb, R. Kalluri, Stage-specific action of matrix metalloproteinases influences progressive hereditary kidney disease, *PLoS Med.* 3 (4) (2006) e100.
- [49] J.M. Catania, G. Chen, A.R. Parrish, Role of matrix metalloproteinases in renal pathophysiology, *Am. J. Physiol. Ren. Physiol.* 292 (3) (2007) F905–F911.
- [50] Q. Zhou, X. Wu, J. Hu, R. Yuan, Abnormal expression of fibrosis markers, estrogen receptor alpha and stromal derived factor1/chemokine (CXC motif) receptor 4 axis in intrauterine adhesions, *Int. J. Mol. Med.* 42 (1) (2018) 81–90.
- [51] J.M. Berman, Intrauterine adhesions, *Semin. Reprod. Med.* 26 (4) (2008) 349–355.
- [52] J. Hu, B. Zeng, X. Jiang, L. Hu, Y. Meng, Y. Zhu, M. Mao, The expression of marker for endometrial stem cell and fibrosis was increased in intrauterine adhesions, *Int. J. Clin. Exp. Pathol.* 8 (2) (2015) 1525–1534.
- [53] A. Abudukeyoumu, M.Q. Li, F. Xie, Transforming growth factor- β 1 in intrauterine adhesion, *Am. J. Reprod. Immunol.* 84 (2) (2020) e13262.
- [54] A. Conforti, C. Alviggi, A. Mollo, G.D. Placido, A. Magos, The management of Asherman syndrome: a review of literature, *Reprod. Biol. Endocrinol.* 11 (2013) 118.
- [55] M. Sillem, S. Prifti, B. Monga, T. Arsllic, B. Runnebaum, Integrin-mediated adhesion of uterine endometrial cells from endometriosis patients to extracellular matrix proteins is enhanced by tumor necrosis factor alpha (TNF alpha) and interleukin-1 (IL-1), *Eur. J. Obstet. Gynecol. Reprod. Biol.* 87 (2) (1999) 123–127.
- [56] T. Cirpan, M.C. Terek, M. Ulukus, E.C. Ulukus, L. Akman, L. Kanit, Immunohistochemical evaluation of cell proliferation and apoptosis markers in ovaries and uterus of tamoxifen-treated rats, *Int. J. Gynecol. Cancer* 18 (1) (2008) 141–145.

- [57] Q. Cong, B. Li, Y. Wang, W. Zhang, M. Cheng, Z. Wu, X. Zhang, W. Jiang, C. Xu, In vitro differentiation of bone marrow mesenchymal stem cells into endometrial epithelial cells in mouse: a proteomic analysis, *Int. J. Clin. Exp. Pathol.* 7 (7) (2014) 3662–3672.
- [58] B.A. Lessey, S.L. Young, What exactly is endometrial receptivity? *Fertil. Steril.* 111 (4) (2019) 611–617.
- [59] A. Zanatta, A.M. Rocha, F.M. Carvalho, R.M. Pereira, H.S. Taylor, E.L. Motta, E.C. Baracat, P.C. Serafini, The role of the Hoxa10/HOXA10 gene in the etiology of endometriosis and its related infertility: a review, *J. Assist. Reprod. Genet.* 27 (12) (2010) 701–710.
- [60] L. Xia, Q. Meng, J. Xi, Q. Han, J. Cheng, J. Shen, Y. Xia, L. Shi, The synergistic effect of electroacupuncture and bone mesenchymal stem cell transplantation on repairing thin endometrial injury in rats, *Stem Cell Res. Ther.* 10 (1) (2019) 244.
- [61] L. Aghajanova, Update on the role of leukemia inhibitory factor in assisted reproduction, *Curr. Opin. Obstet. Gynecol.* 22 (3) (2010) 213–219.
- [62] L.L. Shuya, E.M. Menkhorst, J. Yap, P. Li, N. Lane, E. Dimitriadis, Leukemia inhibitory factor enhances endometrial stromal cell decidualization in humans and mice, *PLoS One* 6 (9) (2011) e25288.
- [63] C.L. Stewart, P. Kaspar, L.J. Brunet, H. Bhatt, I. Gadi, F. Köntgen, S.J. Abbondanzo, Blastocyst implantation depends on maternal expression of leukaemia inhibitory factor, *Nature* 359 (6390) (1992) 76–79.